Optical Traps for sympathetic Cooling of Ions with ultracold neutral Atoms

J. Schmidt,[1,2] P. Weckesser,[2] F. Thielemann,[2] T. Schaetz,[2] and L. Karpa[2,*]

[1] *Laboratoire Kastler Brossel, UPMC-Sorbonne Universits, CNRS, ENS-PSL Research University, Collge de France, 4 place Jussieu, Paris 75005, France*

[2] *Albert-Ludwigs-Universitt Freiburg, Physikalisches Institut, Hermann-Herder-Strae 3, 79104 Freiburg, Germany*

(Dated: January 12, 2022)

We report the trapping of ultracold neutral Rb atoms and Ba^+ ions in a common optical potential in absence of any radiofrequency (RF) fields. We prepare Ba^+ at 370 μK and demonstrate efficient sympathetic cooling by 100 μK after one collision. Our approach is currently limited by the Rb density and related three-body losses, but it overcomes the fundamental limitation in RF traps set by RF-driven, micromotion-induced heating. It is applicable to a wide range of ion-atom species, and may enable novel ultracold chemistry experiments and complex many-body dynamics.

arXiv:1909.08352v1 [physics.atom-ph] 18 Sep 2019

Ultracold ensembles of ions and atoms have been attracting broad interest across disciplines for more than a decade [1–12]. This is largely owed to the prospects of reaching a temperature regime where phenomena are governed by quantum mechanics, which allows new insights into fundamental physics, as well as control over interactions and chemical reactions. The long-range interaction arising from the polarization of atoms opens up novel pathways to access and control many interesting effects and phenomena, such as Feshbach resonances [13, 14], the formation of novel molecular states [15, 16], as well as applications in quantum information processing [17, 18] and simulations [19]. Reaching ultralow temperatures for both species is favourable, and in most cases a prerequisite [10, 20, 21]. Experiments in hybrid traps, confining ions with RF and atoms with optical fields, have shown that sympathetic cooling is highly efficient in the millikelvin energy range and above [4, 5, 8, 9, 11, 22]. However, it was observed that the presence of RF fields inevitably invokes micromotion-induced heating [2, 10, 21, 23]. The latter is inherent to all RF traps and has precluded access to ultralow collision energies. More recently, promising strategies for specific scenarios have been developed, requiring e.g. Rydberg atoms and ions [17], extremely large ion-atom mass ratios [21, 23, 24] or Rydberg excitations within homonuclear atomic ensembles [25]. Yet a universal approach for reaching deep into the quantum regime of interaction for generic combinations of atom and ion species, or even (higher-dimensional) Coulomb crystals, remains an outstanding challenge.

In this Letter, we demonstrate a generic method based on optical ion trapping [26–31], completely overcoming the limitation imposed by micromotion-induced heating [23]. We use bichromatic optical trapping potentials to simultaneously trap and control ions and neutral atoms. We observe highly efficient sympathetic cooling of single Doppler-cooled $^{138}Ba^+$ ions when immersed in a cloud of ultracold ^{87}Rb atoms. We further demonstrate methods for effectively isolating Ba^+ from parasitic ions. Our results pave the way towards realizations of ion-atom collision experiments in the quantum dominated regime.

We adapt the experimental setup described in [27, 28] to allow for optical trapping of ions and atoms as shown in Fig.1(a). We first initialize the Ba^+ by photoionizing Ba atoms emitted from an oven and trapping the ions in a linear Paul trap (RF trap). It features radial and axial secular frequencies of $\omega^{\mathrm{Ba}^+}_{(r,ax)}/(2\pi) \approx (100, 12.5)$ kHz, where the d.c. electrodes provide the axial confinement. Subsequently, the ions are laser cooled to the Doppler limit of $T_D^{\mathrm{Ba}^+} \approx 370$ μK. We compensate stray electric fields to the level of $E_{str} \leq 7\,\mathrm{mV\,m^{-1}}$ [30, 32], and align two axially overlapped counter-propagating dipole trap laser beams (VIS and NIR) with a Ba^+ confined at the center of the RF trap ($z = 0$ m) [27, 28]. The two beams are operated at wavelengths $\lambda_{VIS} = 532\,\mathrm{nm}$ and $\lambda_{NIR} = 1064\,\mathrm{nm}$ while the beam waist radii of $w_0^{NIR} \approx w_0^{VIS} = 3.7 \pm 0.05$ μm are approximately matched at $z = 0$.

The sequence for studying atom-ion interactions comprises four distinct stages shown in Fig.1(b): preparation, pre-cooling, overlapping and bichromatic phase. The latter ensures transfer of the overlapped ion-atom system from the hybrid trap (RF for Ba^+, NIR and VIS for Rb) to the bichromatic optical dipole traps (biODT) where we turn off the RF fields. In the final detection phase, the survival of Ba^+ in the VIS trap is determined after its transfer back to the RF trap via fluorescence imaging on a charge-coupled device (CCD) camera (see Fig.1(b)). Repeating this experiment yields the trapping probability p_{opt}. A variation of the trap depth U_0 (see Fig. 2(a), left) allows to derive the Ba^+ temperature, T^{Ba^+} [26–30].

We start the preparation phase by loading Rb into a magneto-optical trap (MOT) while spatially separating the initialized Ba^+ from the atom cloud. Here, we add electric offset fields $\Delta E_y \approx 15$ V m^{-1} and $\Delta E_z \approx 0.8$ V m^{-1} relative to the configuration determined during the stray field compensation. The former offset the ion radially (axially) by $\Delta y \approx 30$ μm ($\Delta z \approx 300\,\mu$m). After loading the MOT for about $\Delta t_{MOT} \approx 250$ ms, we first transfer the Rb into a crossed NIR optical trap

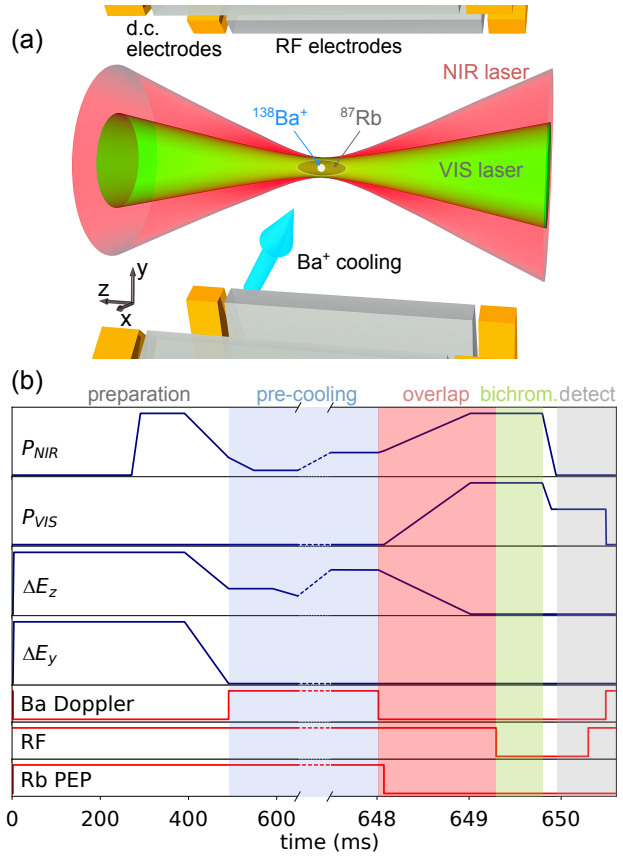


FIG. 1. Schematic of the experimental setup (not to scale) and protocol. **(a)** Bichromatic dipole traps (biODT) comprised of two lasers, VIS and NIR are used to simultaneously trap a ^{138}Ba$^+$ ion and a cloud of ultracold ^{87}Rb atoms. The linear Paul trap (ion-electrode distance: 9 mm) is only employed for preparation and detection of the laser cooled ion (d.c. electrodes for axial confinement, compensation and offset fields). **(b)** Simplified experimental sequence showing the most relevant parameters (scales magnified on the right): $P_{NIR}, P_{VIS}, \Delta E_z, \Delta E_y$ denote the optical powers of the dipole beams and the electric offset fields in the z and y directions. 3 lowermost traces: Ba$^+$ laser cooling (Ba Doppler), RF amplitude (RF), and parametric excitation pulses (PEP). The sequence comprises a preparation (left unshaded), pre-cooling (blue shaded), overlapping (red), interaction (green), and detection phase (grey). During the latter, we detect the survival of Ba$^+$ after trapping in the VIS beam only. Loading the Rb MOT, transfer into a crossed NIR dipole trap and evaporation therein are not depicted.

(not shown in Fig.1), and after 50 ms into a focused NIR dipole trap. Forced evaporation therein yields a cloud of $\sim 10^3$ atoms.

At the end of the preparation phase, we ramp ΔE_y to zero and adjust ΔE_z to position Ba$^+$ about 100 μm away from the trap center ($z = 0$). There, it is Doppler cooled for approximately 150 ms (pre-cooling phase in Fig.1(b)). Subsequently, during the ion-atom overlapping phase in the hybrid trap, the VIS laser is ramped up within $\tau_{ramp} = 1$ ms to $P_{VIS} \approx 470$ mW. This corresponds to an effective trap depth of $U_0/k_B \approx 1.4$ mK for Ba$^+$ (see Fig.2(a), left), where k_B is the Boltzmann constant. Simultaneously, P_{NIR} has to be increased from 26 to 65 mW in order to compensate for the repulsive effect of the VIS laser on Rb (see Fig.2(a), right). This requires maintaining the ratio P_{NIR}/P_{VIS} within a narrow range to keep the trap depth U_0^{Rb} for Rb close to constant (see Fig.2(b,c), right panels)). A deviation by $\sim 10\%$ leads either to substantial heating due to compression by the NIR laser or to atom loss induced by the repulsive VIS laser (see Fig.2(b,c), left panels)). While building up the biODT, the Ba$^+$ is transported to the center of the Rb cloud by ramping ΔE_z to zero. At this point, overlap of Ba$^+$ and Rb in the hybrid trap is established. Note that the biODT deviates from the idealized assumption of circular Gaussian profiles shown in Fig.2(a,b). In our current experimental realization both dipole beams are astigmatic, not perfectly Gaussian and prone to drifts as well as intensity and pointing noise. This causes fluctuations of the number of Rb atoms, their spatial distribution and affects the control of the local density. We illustrate two extreme scenarios in Fig.2(c).

The subsequent bichromatic phase allows for observing ion-atom interactions in absence of RF fields. It is initiated by transferring Ba$^+$ from the RF to the biODT by ramping the RF field to zero. The duration of confinement in the biODT amounts to $\tau \approx 0.5$ ms. The sequence is concluded by ramping the NIR trap to zero, thereby ejecting Rb out of the VIS beam, leaving the ion in the VIS trap. We repeat the sequence to measure p_{opt} and T^{Ba^+}.

So far, we have neglected parasitic ions, assuming that only ^{138}Ba$^+$ was present in the RF trap. However, it has been demonstrated that photo-associative processes at λ_{NIR} within the dense neutral Rb cloud can lead to the formation of Rb$^+$ and Rb_2^+ [33]. This effect is enhanced due to the still large P_{VIS} (and accordingly P_{NIR}) required to initially trap the comparatively hot ion at $T_D^{\mathrm{Ba}^+}$. Both parasitic species fulfil the criteria for stable confinement in our RF trap, as shown for a chain of a single Rb_2^+ and two Ba$^+$ ions in Fig.3 (top left panel). Their disruptive appearance within the cloud leads to heating of Ba$^+$, thereby thwarting its transfer into the shallow biODT. To quantitatively investigate this effect and potential countermeasures, we measure p_{opt} immediately after establishing overlap of Ba$^+$ in the hybrid trap with a cloud of $N \approx (1 \pm 0.15) \times 10^3$ atoms at a temperature of $T^{\mathrm{Rb}} \approx 30 \pm 10$ μK (open squares in Fig.3). We find that p_{opt}, here a measure of transfer efficiency of Ba$^+$ from the hybrid trap to biODT, is consistent with zero for U_0/k_B up to 3 mK. This imposes a lower bound on the kinetic energy in the range of several $k_B \times$ mK. In our case, the parasitic ions have to be selectively removed from the hybrid trap prior to overlapping Ba$^+$ with the now purified Rb ensemble. To this end we apply ΔE_z

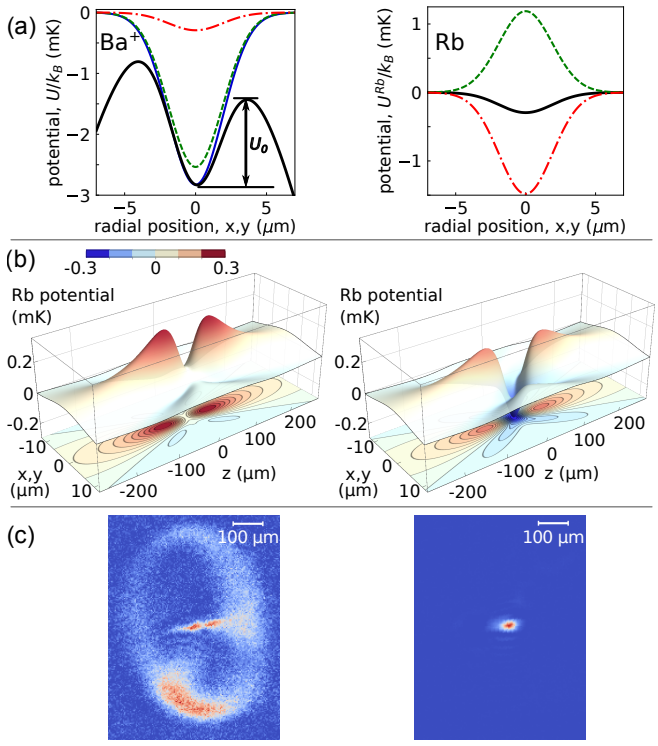


FIG. 2. Bichromatic trapping potentials for Ba^+ and Rb. **(a)** (left) Calculated optical potential for Ba^+ at $z = 0$ (blue, solid) with VIS (green, dashed) and NIR (red, dash-dotted) contributions. Taking into account electrostatic defocusing and stray fields (black, thick) yields an effective trap depth of $U_0/k_B \approx 1.4$ mK. (right) Calculated bichromatic potential for Rb (solid, black) with the repulsive VIS and attractive NIR potentials adjusted to provide an effective trap depth of $U_0^{\mathrm{Rb}} = U_{NIR}^{\mathrm{Rb}}(x, y = 0) + U_{VIS}^{\mathrm{Rb}}(x, y = 0) \approx k_B \times 300\ \mu$K within the $z = 0$ plane. **(b)** Corresponding bichromatic potential landscape for Rb (contour plot at the bottom). (left) In the unbalanced case $\left|U_{VIS}^{\mathrm{Rb}}\right| > \left|U_{NIR}^{\mathrm{Rb}}\right|$: the potential at $z = 0$ is rendered repulsive featuring shallow lobes around $z \approx \pm 50\ \mu$m. (right) In the balanced case $U_0^{\mathrm{Rb}}/k_B \approx 300\ \mu$K, the global minimum is located at the center. **(c)** Absorption images of Rb ($N \approx 4 \times 10^3$ atoms) in a bichromatic potential after $\sim 100\ \mu$s time-of-flight taken nearly from the x direction (projecting into the $y - z$ plane): (left) VIS ramp is leading with respect to the NIR ramp and (right) with appropriately synchronized ramp-up of P_{VIS} and P_{NIR}. In the unbalanced case, atoms have been ejected from the center, while some atoms still accumulate at the local minima around $z \approx \pm 50\ \mu$m.

and ΔE_y to offset Ba^+ in combination with a series of chirped parametric excitation pulses (PEP). That is, we modulate the amplitude of the RF field at twice the radial secular frequencies of both the Rb^+ and Rb_2^+ (sweep of ± 5, and ± 2.5 kHz, respectively) [33]. As shown in Fig.3(top), this method efficiently removes the parasitic ions, even if they are embedded into a Ba^+ Coulomb crystal. The measured p_{opt} reveals an improved transfer and trapping performance to $p_{opt} \approx 0.8$ (see blue circles in Fig.3). We account for $p_{opt} < 1$ by considering the finite maximal p_{opt} in the radial-cutoff model [31]. A fit to the data with the adapted model yields a temperature of $T_{init}^{\mathrm{Ba}^+} = 356 \pm 30\,\mu$K. This is consistent with $T_D^{\mathrm{Ba}^+}$. We conclude that the reduced transfer efficiency is due to loss of Ba^+ rather than heating. The observed loss could be caused e.g. by a residual survival probability of motionally excited Rb^+ or Rb_2^+ on larger orbits within the RF trap or by motional excitation of Ba^+ during the transport phases with amplitudes exceeding the effective range of the pre-cooling lasers. Notwithstanding, PEP combined with a laser pre-cooling phase (see Fig.1(b)) efficiently isolates Ba^+ at the end of the overlapping sequence.

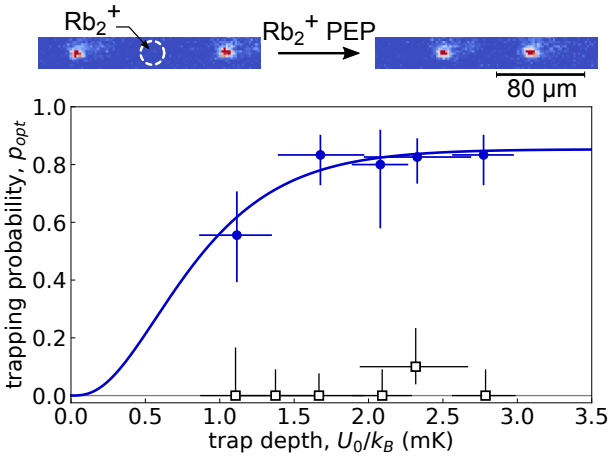


FIG. 3. Isolation efficiency of Ba^+ from parasitic ions before transfer into the bichromatic trap. Optical trapping probability p_{opt} in the VIS trap of depth U_0/k_B at the end of the overlapping phase without (black hollow squares) and with parametric excitation pulses (PEP) applied during loading and evaporation of Rb. Error bars: (trap depth) upper bounds of 1 σ uncertainties extracted from bootstrapping; (p_{opt}) 1 σ confidence intervals calculated from the underlying binomial distribution. (top) Three-ion chain with a Rb_2^+ molecule embedded in a Ba^+ crystal before (left) and after (right) application of PEP tuned in resonance with Rb_2^+, selectively removing the parasitic ion [33]. In our experiment: Rb and Ba^+ are spatially separated while PEP is active, such that Rb^+ and Rb_2^+ ions are expelled before crystallizing.

We now study the interaction of Ba^+, pre-cooled to $T_D^{\mathrm{Ba}^+}$, and Rb within the hybrid trap in dependence on the duration of overlap τ_{hyb}. Even for well compensated E_{str}, we observe that Ba^+ experiences heating. For τ_{hyb} on the order of ms and atomic densities of $n_0 \sim 10^{12}\,\mathrm{cm}^{-3}$ we measure a heating rate $R_{RF} = 0.3 \pm 0.14\,\mathrm{K\,s}^{-1}$. In contrast, in absence of Rb, R_{RF} remains below our detection limit. We attribute the former to micromotion-induced heating, in agreement with previous results obtained in hybrid traps [10].

We finally investigate the interaction of Ba^+ and Rb within the biODT. We carry out the complete experi-

mental sequence, now including the bichromatic phase with a duration τ_{int}. To distinguish the impact of the ion-atom interaction from any systematic effects, we either keep the Rb, or dismiss it directly after transferring Ba^+ into the biODT. We start this stage of the sequence by confining $N \approx 500 \pm 150$ Rb in the biODT and turn off the RF trap while the d.c. voltages remain constant. This transfers the $Ba^+ - Rb$ ensemble into the biODT. To establish reference conditions by dismissing the Rb, we illuminate the ensemble with laser pulses resonant with the $5\ ^2S_{1/2} \rightarrow 5\ ^2P_{3/2}$ transition in ^{87}Rb which do not affect Ba^+. After $\tau_{int} \approx 0.5$ ms with the Ba^+ in the biODT, we ramp P_{NIR} to zero and measure p_{opt} for Ba^+ in the VIS trap. The results of these reference measurements are shown as red data points (open squares) in Fig.4. We recover the maximal p_{opt} of approximately 0.8, revealing that the transfer efficiency from the hybrid trap into the biODT remains comparable to the results presented in Fig.3. By fitting the data with the adapted cutoff model, we derive a temperature of $T_{init}^{Ba^+} = 357 \pm 22\,\mu$K, in agreement with both the result of Fig.3 and $T_D^{Ba^+}$.

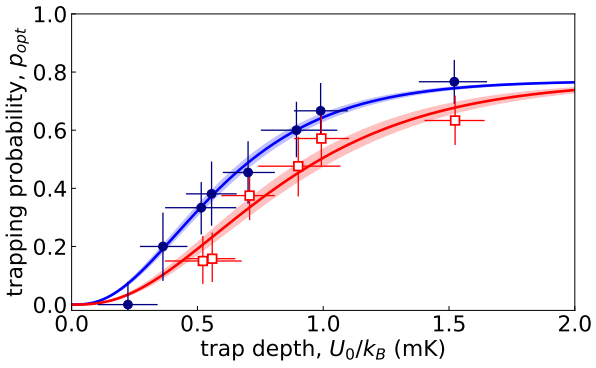


FIG. 4. Sympathetic cooling of a Ba^+ ion in a cloud of ultracold Rb atoms. Open squares: experimental data taken after placing the ion in the bichromatic trap in absence of atoms. An orthogonal distance regression fit with a modified radial cutoff model [31] to the data (lower solid line) yields a temperature of $T_{init}^{Ba^+} = 357 \pm 22\,\mu$K. Full circles: the same experiment carried out with atoms. A fit to the data (upper solid line) yields $T_{symp}^{Ba^+} = 259 \pm 10\,\mu$K, showing evidence for sympathetic cooling below the Doppler limit $T_D^{Ba^+}$. Shaded regions: bounds corresponding to the fit standard errors. Error bars: (trap depth) upper bounds of 1 σ uncertainties extracted from bootstrapping; (p_{opt}) upper bounds of 1 σ confidence intervals calculated from the underlying binomial distribution.

We now repeat this experiment but maintain the overlap of Ba^+ with the Rb atoms during the bichromatic phase. In presence of a Rb ensemble in the biODT we observe a significant increase of p_{opt} as shown in Fig.4 (blue circles). The corresponding temperature amounts to $T_{symp}^{Ba^+} = 259 \pm 10\,\mu$K. That is, we demonstrate the onset of sympathetic cooling of Ba^+, reducing the energy by $k_B \Delta T_{symp} = k_B(-98 \pm 24)\ \mu$K through interaction with the surrounding ensemble of Rb atoms. This result is in good agreement with our estimation of the Langevin collision rate of $\gamma_{Lgvn} \approx 1.5 \pm 0.4 \times 10^3\,\mathrm{s}^{-1}$ (Rb density of $n_0 \approx 5 \times 10^{11}\,\mathrm{cm}^{-3}$) based on the measured average atom temperature and interaction duration [34]. This corresponds to, on average, one Langevin collision. Our finding indicates that the sympathetic cooling mechanism is highly efficient with a measured rate of $R_{symp} = -196 \pm 48$ mK s^{-1}, removing about a third of the ion's kinetic energy after a single interaction event.

We note that in our current parameter regime, we still face restrictions attributed to residual photo-assisted ionization of neutral rubidium and three-body recombination processes in the bichromatic trap. Shot-to-shot fluctuations of trap overlap and the resulting atomic densities currently limit the accessible interaction time to the range of ms [35]. This is three orders of magnitude shorter than the obtainable lifetimes in our apparatus [27]. Prolonged τ_{int} would allow to significantly reduce atom densities, suppressing the three-body loss rate scaling as $\gamma_{3b} \propto n_0^2$, whereas the density dependence of the Langevin rate is $\gamma_{Lgvn} \propto n_0$. In our system, approximately 10 collision events are predicted to be sufficient for reaching thermal equilibrium of Ba^+ with an ultracold Rb ensemble [36]. Here, $T^{Rb} \approx 30\ \mu$K in the biODT due to conservatively chosen parameters to ensure $n_0 < 10^{12}$ cm^{-3} and correspondingly moderate γ_{3b}. Note that in our NIR trap, quantum degenerate ensembles also have been achieved. With our approach the ion energy is expected to obey the Boltzmann distribution, in contrast to the non-thermal distributions observed in hybrid traps [37–39]. This may be advantageous for experiments in the quantum regime. Dipole trap lasers operated at optimized detunings and initialization of the ion at sub-Doppler temperatures [10, 40] would allow to substantially decrease the optical intensity initially required to trap the Ba^+ ion, reducing the generation rates of Rb^+/Rb_2^+ ions. Similarly, using a different element, such as fermionic ^{6}Li, may allow to precool Ba^+ to lower energies in the hybrid trap according to theoretical predictions [23] or, as recently demonstrated, for the $^6\mathrm{Li} - ^{171}\mathrm{Yb}^+$ system [24]. With the outlined technical improvements, thermal equilibration of Ba^+ and Rb should be within reach in the current setup. Another approach to address the limitations arising from three-body recombination would be to either tune the scattering length by utilizing Feshbach resonances [41, 42] or to employ fermionization by preparing a one-dimensional gas of Rb atoms [43].

To summarize, we have demonstrated a method for preparing, overlapping and observing the interactions between ions and neutral atoms in an optical trap while maintaining isolation from parasitic ions. The complete absence of RF fields eliminates micromotion-induced heating, a long-standing obstacle for observing ultracold

ion-atom interactions in hybrid traps [23]. We have further shown sympathetic cooling of Ba^+ below its initial Doppler temperature. Furthermore, our approach is not limited to extremely large ion-atom mass ratios, Rydberg atoms or homonuclear samples and may provide a generic method for establishing interactions between atoms and ion(s) in the s-wave scattering regime, even in higher dimensional crystalline structures.

This project has received funding from the European Research Council (ERC) under the European Unions Horizon 2020 research and innovation program (Grant No. 648330). J. S., F. T. and P. W. acknowledge support from the DFG within the GRK 2079/1 program. P. W. gratefully acknowledges financial support from the Studienstiftung des deutschen Volkes. We are indebted to V. Vuletić, D. Leibfried, R. Moszynski, M. Tomza and O. Dulieu for many fruitful discussions.

* leon.karpa@physik.uni-freiburg.de

[1] W. W. Smith, O. P. Makarov, and J. Lin, Cold ion-neutral collisions in a hybrid trap, Journal of Modern Optics **52**, 2253 (2005), https://doi.org/10.1080/09500340500275850.

[2] A. T. Grier, M. Cetina, F. Oručević, and V. Vuletić, Observation of Cold Collisions between Trapped Ions and Trapped Atoms, Phys. Rev. Lett. **102**, 223201 (2009).

[3] S. Schmid, A. Härter, and J. H. Denschlag, Dynamics of a Cold Trapped Ion in a Bose-Einstein Condensate, Phys. Rev. Lett. **105**, 133202 (2010).

[4] C. Zipkes, S. Palzer, C. Sias, and M. Köhl, A trapped single ion inside a Bose-Einstein condensate, Nature **464**, 388 (2010).

[5] K. Ravi, S. Lee, A. Sharma, G. Werth, and S. Rangwala, Cooling and stabilization by collisions in a mixed ion-atom system, Nature Communications **3**, 1126 (2012).

[6] F. H. J. Hall and S. Willitsch, Millikelvin Reactive Collisions between Sympathetically Cooled Molecular Ions and Laser-Cooled Atoms in an Ion-Atom Hybrid Trap, Phys. Rev. Lett. **109**, 233202 (2012).

[7] W. G. Rellergert, S. T. Sullivan, S. Kotochigova, A. Petrov, K. Chen, S. J. Schowalter, and E. R. Hudson, Measurement of a Large Chemical Reaction Rate between Ultracold Closed-Shell ^{40}Ca Atoms and Open-Shell ^{174}Yb Ions Held in a Hybrid Atom-Ion Trap, Phys. Rev. Lett. **107**, 243201 (2011).

[8] A. Härter and J. H. Denschlag, Cold atom–ion experiments in hybrid traps, Contemporary Physics **55**, 33 (2014).

[9] S. Haze, M. Sasakawa, R. Saito, R. Nakai, and T. Mukaiyama, Cooling Dynamics of a Single Trapped Ion via Elastic Collisions with Small-Mass Atoms, Physical Review Letters **120**, 043401 (2018).

[10] Z. Meir, T. Sikorsky, R. Ben-shlomi, N. Akerman, Y. Dallal, and R. Ozeri, Dynamics of a Ground-State Cooled Ion Colliding with Ultracold Atoms, Phys. Rev. Lett. **117**, 243401 (2016).

[11] M. Tomza, K. Jachymski, R. Gerritsma, A. Negretti, T. Calarco, Z. Idziaszek, and P. S. Julienne, Cold hybrid ion-atom systems, Rev. Mod. Phys. **91**, 035001 (2019).

[12] J. Deiglmayr, A. Göritz, T. Best, M. Weidemüller, and R. Wester, Reactive collisions of trapped anions with ultracold atoms, Phys. Rev. A **86**, 043438 (2012).

[13] Z. Idziaszek, T. Calarco, P. S. Julienne, and A. Simoni, Quantum theory of ultracold atom-ion collisions, Phys. Rev. A **79**, 010702 (2009).

[14] M. Tomza, C. P. Koch, and R. Moszynski, Cold interactions between an Yb $^+$ ion and a Li atom: Prospects for sympathetic cooling, radiative association, and Feshbach resonances, Phys. Rev. A **91**, 10.1103/physreva.91.042706 (2015).

[15] R. Côté, V. Kharchenko, and M. D. Lukin, Mesoscopic Molecular Ions in Bose-Einstein Condensates, Phys. Rev. Lett. **89**, 093001 (2002).

[16] J. M. Schurer, A. Negretti, and P. Schmelcher, Unraveling the Structure of Ultracold Mesoscopic Collinear Molecular Ions, Physical Review Letters **119**, 1 (2017).

[17] T. Secker, R. Gerritsma, A. W. Glaetzle, and A. Negretti, Controlled long-range interactions between Rydberg atoms and ions, Phys. Rev. A **94**, 013420 (2016).

[18] H. Doerk, Z. Idziaszek, and T. Calarco, Atom-ion quantum gate, Phys. Rev. A **81**, 012708 (2010).

[19] U. Bissbort, D. Cocks, A. Negretti, Z. Idziaszek, T. Calarco, F. Schmidt-Kaler, W. Hofstetter, and R. Gerritsma, Emulating Solid-State Physics with a Hybrid System of Ultracold Ions and Atoms, Phys. Rev. Lett. **111**, 080501 (2013).

[20] M. Krych, W. Skomorowski, F. Pawłowski, R. Moszynski, and Z. Idziaszek, Sympathetic cooling of the Ba^+ ion by collisions with ultracold Rb atoms: Theoretical prospects, Phys. Rev. A **83**, 032723 (2011).

[21] H. A. Fürst, N. V. Ewald, T. Secker, J. Joger, T. Feldker, and R. Gerritsma, Prospects of reaching the quantum regime in Li-Yb^+ mixtures, Journal of Physics B: Atomic, Molecular and Optical Physics **51**, 195001 (2018), arXiv:1804.04486.

[22] I. Sivarajah, D. S. Goodman, J. E. Wells, F. A. Narducci, and W. W. Smith, Evidence of sympathetic cooling of Na^+ ions by a Na magneto-optical trap in a hybrid trap, Phys. Rev. A **86**, 063419 (2012).

[23] M. Cetina, A. T. Grier, and V. Vuletić, Micromotion-Induced Limit to Atom-Ion Sympathetic Cooling in Paul Traps, Phys. Rev. Lett. **109**, 253201 (2012).

[24] T. Feldker, H. Fürst, H. Hirzler, N. V. Ewald, M. Mazzanti, D. Wiater, M. Tomza, and R. Gerritsma, Buffer gas cooling of a trapped ion to the quantum regime, **8**, 1 (2019), arXiv:1907.10926.

[25] K. S. Kleinbach, F. Engel, T. Dieterle, R. Löw, T. Pfau, and F. Meinert, Ionic Impurity in a Bose-Einstein Condensate at Submicrokelvin Temperatures, Phys. Rev. Lett. **120**, 193401 (2018).

[26] C. Schneider, M. Enderlein, T. Huber, and T. Schaetz, Optical trapping of an ion, Nature Photonics **4**, 772 (2010).

[27] A. Lambrecht, J. Schmidt, P. Weckesser, M. Debatin, L. Karpa, and T. Schaetz, Long lifetimes and effective isolation of ions in optical and electrostatic traps, Nat. Photonics **11**, 704 (2017).

[28] J. Schmidt, A. Lambrecht, P. Weckesser, M. Debatin, L. Karpa, and T. Schaetz, Optical Trapping of Ion Coulomb Crystals, Phys. Rev. X **8**, 021028 (2018), arXiv:1712.08385.

[29] T. Schaetz, Trapping ions and atoms optically, Journal

of Physics B: Atomic, Molecular and Optical Physics **50**, 102001 (2017).

[30] L. Karpa, *Trapping single ions and Coulomb crystals with light fields* (SpringerBriefs in Physics (in press), 2019).

[31] C. Schneider, M. Enderlein, T. Huber, S. Dürr, and T. Schaetz, Influence of static electric fields on an optical ion trap, Phys. Rev. A **85**, 013422 (2012).

[32] T. Huber, A. Lambrecht, J. Schmidt, L. Karpa, and T. Schaetz, A far-off-resonance optical trap for a Ba^+ ion, Nature Communications **5** (2014).

[33] A. Härter, A. Krükow, M. Deiß, B. Drews, E. Tiemann, and J. H. Denschlag, Population distribution of product states following three-body recombination in an ultracold atomic gas, Nat. Phys. **9**, 512 (2013).

[34] B. Höltkemeier, P. Weckesser, H. López-Carrera, and M. Weidemüller, Buffer-gas cooling of a single ion in a multipole radio frequency trap beyond the critical mass ratio, Phys. Rev. Lett. **116**, 233003 (2016).

[35] A. Krükow, A. Mohammadi, A. Härter, J. H. Denschlag, J. Pérez-Ríos, and C. H. Greene, Energy Scaling of Cold Atom-Atom-Ion Three-Body Recombination, Phys. Rev. Lett. **116**, 10.1103/physrevlett.116.193201 (2016).

[36] H. Metcalf and P. Van der Straten, *Laser Cooling and Trapping* (Springer, 1999).

[37] R. G. DeVoe, Power-Law Distributions for a Trapped Ion Interacting with a Classical Buffer Gas, Phys. Rev. Lett. **102**, 063001 (2009).

[38] Z. Meir, M. Pinkas, T. Sikorsky, R. Ben-shlomi, N. Akerman, and R. Ozeri, Direct Observation of Atom-Ion Nonequilibrium Sympathetic Cooling, Phys. Rev. Lett. **121**, 53402 (2018).

[39] I. Rouse and S. Willitsch, Superstatistical Energy Distributions of an Ion in an Ultracold Buffer Gas, Phys. Rev. Lett. **118**, 143401 (2017), arXiv:1703.06006.

[40] L. Karpa, A. Bylinskii, D. Gangloff, M. Cetina, and V. Vuletić, Suppression of Ion Transport due to Long-Lived Subwavelength Localization by an Optical Lattice, Phys. Rev. Lett. **111**, 163002 (2013).

[41] S. L. Cornish, N. R. Claussen, J. L. Roberts, E. A. Cornell, and C. E. Wieman, Stable ^{85}Rb Bose-Einstein Condensates with Widely Tunable Interactions, Phys. Rev. Lett. **85**, 1795 (2000).

[42] E. A. Donley, N. R. Claussen, S. L. Cornish, J. L. Roberts, E. A. Cornell, and C. E. Wieman, Dynamics of collapsing and exploding Bose-Einstein condensates, in *Collect. Pap. Carl Wieman* (WORLD SCIENTIFIC, 2008) pp. 612–616.

[43] J. Goold, H. Doerk, Z. Idziaszek, T. Calarco, and T. Busch, Ion-induced density bubble in a strongly correlated one-dimensional gas, Phys. Rev. A **81**, 041601 (2010).